Velocity Measurements in Cardiac Magnetic Resonance Imaging

Rolf, M.P.

2012

document version
Publisher's PDF, also known as Version of record

Chapter 1

Introduction

Magnetic Resonance Imaging (MRI) is a fascinating technique to visualize the interior of the human body. My fascination originates from the multitude of physical principles that the technique is based on and the multitude of anatomical and physiological information that can be gained from it. This introduction starts to give a general idea of the physical principles (§1.1), on which the research described in this thesis, is based and which clinical perspective (§1.2) was kept in mind. In §1.3, a more detailed explanation on MRI velocity measurements is given together with an outline of the thesis.

1.1 Magnetic Resonance Imaging

Magnetic Resonance Imaging is a complex technique. The two main concepts that will be described in this section are, firstly, the creation of a signal from nuclear resonance in the presence of a magnetic field, and secondly the localization of the created signal to construct an image.

Nuclear Magnetic Resonance
MRI signal is created from the magnetic properties of the hydrogen nuclei (protons) in water. The magnetic properties of the proton follow from the quantum mechanical spin-$\frac{1}{2}$ property, therefore the protons are often referred to as 'spins'. To influence the spins a MR scanner makes use of a very strong magnet (see Figure 1.1). All the hydrogen nuclei will be aligned either parallel or anti-parallel to the strong magnetic field. There are a few more spins that align parallel than anti-parallel, resulting in a net magnetization in the direction of the external magnetic field. The nuclei do not align perfectly, but they rotate around the main direction (precession) as is illustrated in Figure 1.2. The frequency with which they precess depends linearly on the strength of the magnetic field, typically this frequency is in the range of the radio frequencies (RF). Using an external electromagnetic pulse in the radio frequency range (RF-pulse), the spins can be excited. The excited spins will generate a resonance signal, and it is this resonance signal that is utilized.

After the RF-pulse is turned off, the spins will return to their equilibrium state. This relaxation process is accelerated by the chemical environment of the spin (stimulated emission). Tissues in the body can be characterized by their differences in chemical composition, and can be distinguished due to differences in relaxation times. There are two tissue-parameters by which the relaxation process can be characterized. Firstly, there is the spin-lattice interaction. The more the water is bound in a tissue, the easier energy can be transferred to the lattice and the faster the excited spins will return to their equilibrium state. Secondly, there is the spin-spin interaction. The small magnetic fields of the spins can disturb each other when they are lo-

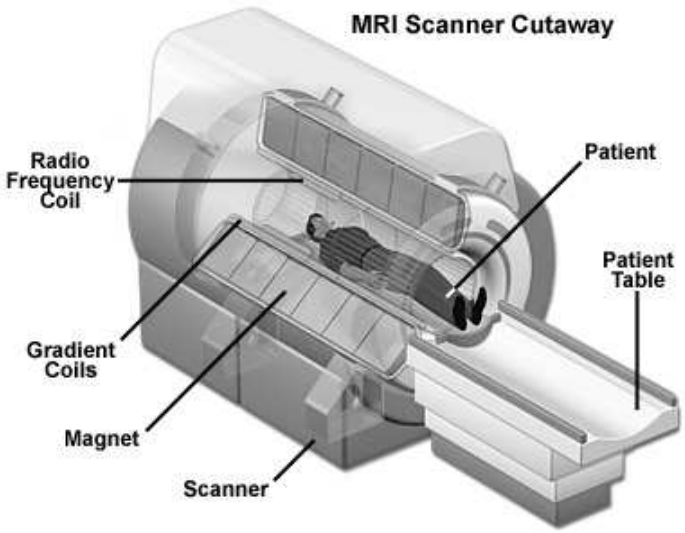

Figure 1.1: MR scanner cut-away showing the main magnet for alignment of the spins, the radio frequency coil for excitation, and the gradient coils for localization.
Source: www.magnet.fsu.edu/education/tutorials/magnetacademy

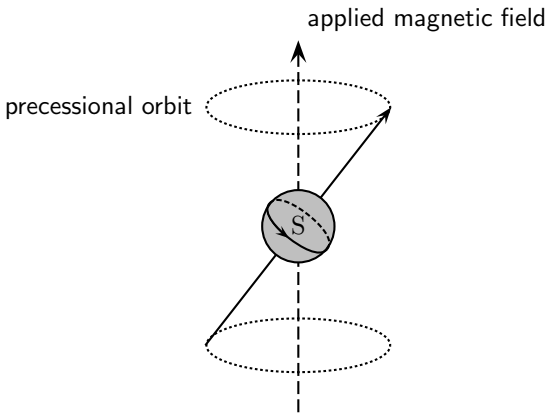

Figure 1.2: The nucleus' rotational axis precesses in an orbit around the applied magnetic field.

cated close together, thereby loosing their synchronism of rotation. The more synchronisity is lost the less net resonance signal remains. Both relaxation processes exhibit an exponential behavior, which can be characterized by a single time constant. The time constants with which these two processes take place are called T1 (spin-lattice) and T2 (spin-spin). T1 and T2 are to some extent independent of each other and are together specific for many different tissues.

The MR signal originates from the resonance of spins, and contrast between tissues is due to differences in the proton density, and the T1 and T2 relaxation times. Therefore timing is an important parameter: Firstly, the time between successive excitation RF-pulses, time of repetition (TR), interacts with the spin-lattice relaxation (T1) as only non-excited spins are available for excitation. Secondly, the time between excitation and reception of the signal, time of echo (TE), interacts with the spin-spin relaxation (T2) as the amount of synchronicity determines the strength of the net signal. By tuning the technical parameters TR and TE to the tissue parameters T1 and T2, the signal contrast between tissues can be adjusted.

This technique was originally named Nuclear Magnetic Resonance (NMR) [1, 2], and is still a powerful tool in (non-destructive) chemical analysis.

MR Imaging

To create an image one has to know the position where the signal originates from. The magnet in the scanner is designed to generate a homogeneous magnetic field, B_0, in the center of the scanner. As the rotation frequency of the spins depends on the strength of the magnetic field, all spins within the B_0-field will start to resonate at excitation, irrespective of their position. By adding a small magnetic field that varies with position, the resonance frequency will vary with position, opening up the way towards localization. These additional magnetic fields vary linearly in one direction and are therefore called 'gradient' fields. MR scanners contain hardware to create three orthogonal gradient fields, any combination of these gradient fields creates an oblique gradient field.

By applying a gradient field simultaneously with the RF-pulse, only spins in a certain slice, perpendicular to the gradient field, will be excited (slice selection, SS). This slice will form the image plane. As addition of other gradient fields will only generate an oblique slice, signal localization within the image plane has to be effected in another way. Applying a gradient field after excitation will adapt the resonance frequency of the spins to the local magnetic field strength. This way the resonance signal will consist of a whole spectrum of frequencies in which information about the spatial position is encoded. As gradient fields still can only be applied in one direction, the experiment has to be repeated for each encoding in the second in-plane direction. These two in-plane encodings are referred to as frequency (or read-out) encoding (FE or RO) and phase encoding (PE). With the combination of these two encodings a spatially-dependent resonance frequency spectrum is created. This spatial frequency spectrum is also called k-space. Data from k-space can be reconstructed by 2D Fourier transform to spatial positions, the image. In k-space every data point contains information about every pixel in the final image, important to note is that this causes a complex but typical relation with artifacts from acquisition errors.

The whole entirety of excitation RF pulse, applied gradient fields, signal read-out and their timing details is called a 'sequence'. MRI sequences exist in many varieties, each variety has its distinct features on image quality, tissue contrast, acquisition time and artifact behavior. An example of an MRI sequence is shown in Figure 1.3. At this point where the NMR technique became suitable for medical diagnostic imaging the name was changed to Magnetic Resonance Imaging [3–6].

1.2 Cardiac MRI

A growing area of MRI applications is non-invasive diagnostic cardiology [7–10]. The possibility of imaging slices in any oblique orientation is especially useful in the heart as it is positioned obliquely in the chest. Over the years, gradient systems have become stronger and

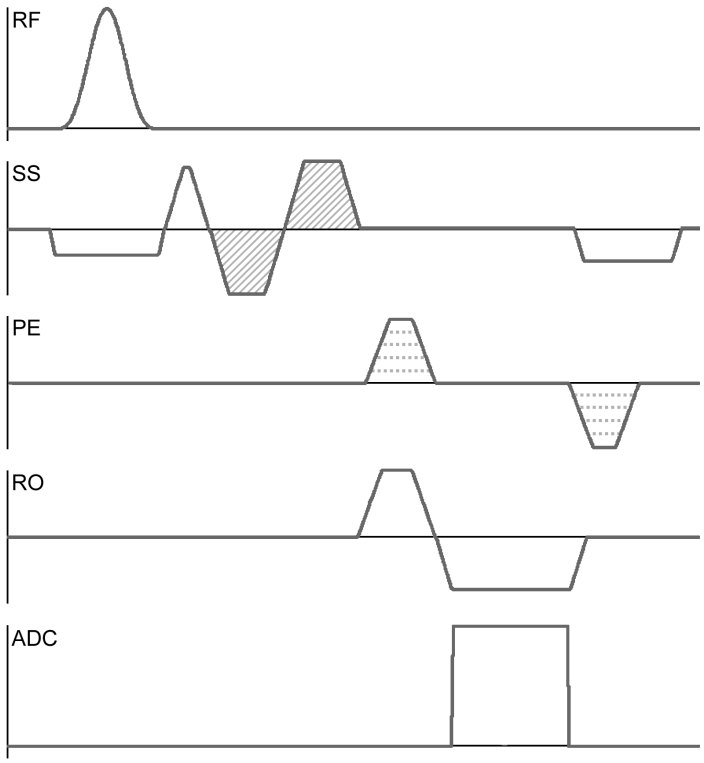

Figure 1.3: An example of an MRI sequence. The relative time is indicated horizontally. The upper axis (RF) shows the strength and duration of the RF excitation pulse. The slice selection gradients (SS) are switched on simultaneous with the RF-pulse. Phase encoding (PE) and read-out (RO) gradients are shown in the next two axes. The dotted lines in the PE gradients indicate the phase encoding steps to be repeated over several TR's. The last axis (ADC) indicates when MR signal is recorded. The bipolar gradient (hatched) for velocity encoding is applied on the SS-axis. One repetition time (TR) is shown.

faster. Imaging became fast enough to take physiological processes as breathing and beating of the heart into account. This facilitated imaging during a breath-hold of the patient and gave enough temporal resolution to reconstruct images into a movie ('cine') showing several phases of the cardiac cycle.

Besides imaging the anatomy by tissue contrast, the MR technique also has the capability of measuring velocities of moving spins [11–14]. This can be applied to measure the velocity of blood flow through the heart and arteries. The physical principles and technical aspects of velocity measurements will be discussed in the next section, first the application in cardiology will be further explained.

The heart (Figure 1.4) can be considered as a pump supporting the blood circulation, therefore its function can be assessed by measurement of the blood volumes flowing through it. The most straight forward measurement for this purpose is to measure the amount of blood that is pumped out of the heart, the cardiac output [15, 16]. Aortic and pulmonary artery flow measurements and differences in flow between the two can provide valuable insight in cardiac output, shunt flow (abnormal flow between the venous and arterial circulation), and aortic and pulmonary regurgitation due to valvular insufficiencies (backward flow).

Mitral Valve

The heart is a one-way pump and therefore has valves to prevent the blood from flowing backwards (see Figure 1.4). The valve situated between the left atrium and the left ventricle is the mitral valve. Through various causes the two leaflets of the mitral valve can become defective. Rheumatic fever, valve prolapse, infective endocarditis, myocardial dysfunction, and papillary muscle dysfunction are for example among these causes [17]. A defective valve can leak blood in the backward direction, called regurgitation, and places an extra workload on the heart. If severe, this extra workload can eventually cause congestive heart failure [17]. An accurate measurement of the regurgitant volume will aid the physician in decision making about treatment.

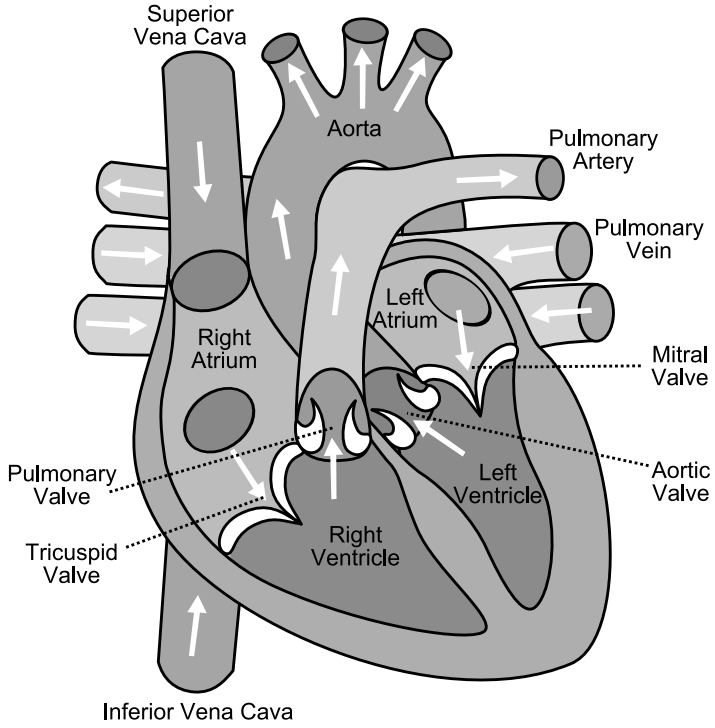

Figure 1.4: The human heart. Blood returns from the body via the vena cavae into the right atrium, from there through the tricuspid valve into the right ventricle. From the right ventricle the blood is pumped into the lungs through the pulmonary artery. From the lungs the blood returns via the pulmonary veins into the left atrium, and through the mitral valve into the left ventricle. From the left ventricle the blood is pumped into the systemic circulation starting in the aorta. Source: http://en.wikipedia.org/wiki/Cardiovascular_system

A current area of investigation is flow quantification through the mitral valve, especially in the case of mitral regurgitation [18–20]. For non-invasive diagnostics in cardiology the most widely available imaging technique is echocardiography [21]. Echocardiographic velocity measurements using Doppler techniques are quantitative. However, the Doppler samples can not be measured accurately at multiple locations in the valvular plane, reliable integration to a volume-flow is therefore not possible. Thus, the amount of mitral valve leakage can only be categorized semi-quantitatively into four categories: none, mild, moderate, and severe. Furthermore, echocardiography depends on a good 'acoustic window': ribs, lungs, and abdominal fat may hamper a good view on the heart. Echocardiography is therefore not an optimal technique for accurate quantification and/or monitoring of disease progression.

MRI is capable of accurate quantitative velocity measurements in combination with an unobstructed view on the heart. Aortic and pulmonary valve regurgitation can be accurately measured directly downstream of the valve. The mitral valve, however, moves considerably through the cardiac cycle [19, 22]. The current approach for mitral regurgitation is therefore an indirect one: aortic cardiac output measurements are compared with left ventricle volume changes from anatomical images [15, 23]. The difference in blood volume between the forward aortic flow volume and the stroke volume derived from end-diastolic and end-systolic ventricular volume measurements yields the backward flow through the mitral valve. A disadvantage of this method is its sensitivity to errors, as two large volumes are subtracted to calculate a small volume. A direct quantification method should be adapted to or incorporate the valvular motion, which is technically challenging [22]. The technical aspects of direct velocity quantification at the mitral valve will be presented in more detail in the next section.

1.3 Velocity Measurements

Resonating spins that are moving during application of a gradient, change resonance frequency along with the local resonance frequency. This effect can be unwanted and leading to artifacts in the resulting image, but can also be used in advantage to measure the movement.

After application of a gradient, the moving spins will have the same frequency as their new stationary neighbors, but because of their different history of rotations the moving spins will be in another phase of their rotation. This phase deviation is directly proportional to the velocity of the spins (assuming constant velocity). If this gradient is followed by an equal gradient but with opposite polarity (of the small additional magnetic field), the stationary spins will have the same phase as before the gradients were applied. This implies that applying two equal gradients with opposite polarity, a bipolar gradient, will not interfere with the imaging process, but moving spins will have acquired a phase deviation proportional to their velocity. Unfortunately, the phase of stationary spins is still undefined as there are other phenomena that also introduce phase changes. The arbitrary phases from sources insensitive to gradients and constant over time can easily be eliminated by subtraction of two measurements, one with the velocity encoding bipolar gradient, and one without. The phases from gradient-depending sources are not easy to eliminate, these will be discussed later in this section. The bipolar gradient can be applied in each of the three imaging directions (SS, RO, FE), resulting in velocity measurements in each of these specific directions: through-plane, and/or in-plane. This way of MR velocity measurement is referred to as the 'phase contrast' (PC) technique [11–13]. A phase contrast sequence is shown in Figure 1.3.

Phase signals are only unique over one rotation, which translates into a finite range of velocities that are uniquely identifiable. This range depends on the strength and timing of the bipolar gradient and is indicated by the parameter v_{enc}. Besides the phase, the magnitude of the measured signal contains still the normal tissue information. Therefore the result of a phase contrast measurement will normally be presented in two images; a magnitude image, showing the anatomy by

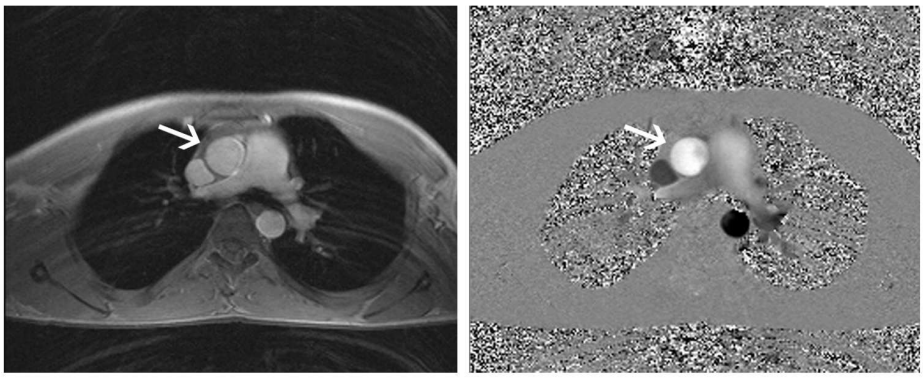

Figure 1.5: Magnitude image showing the anatomy and the accompanying phase map with through-plane velocity measurements in a transverse plane just above the heart. The aorta ascendens is indicated by the white arrows. Grey indicates zero velocity, white velocities in one direction (in this case towards the head) and black in the opposite direction (towards the feet).

tissue contrast, and a phase map, representing velocities. An example of a magnitude image and its accompanying phase map is shown in Figure 1.5.

As any other technique, also phase contrast imaging has its limitations. Two issues of interest for cardiac MRI will be investigated and discussed in this thesis. The following section will give an introduction on the background of these issues and an overview of the research that has been conducted in these areas.

1.4 Aim of study

Part I - Flow quantification of the mitral valve: combining phase contrast with SSFP sequences

Mitral valve regurgitation assessment is challenging because of the constant valvular movement, as was pointed out earlier. These circumstances require a velocity measurement in a 3D spatial volume,

with velocity sensitivity in all three orthogonal directions and time resolved (7-dimensional). On current commercially available MR-scanners, the phase-contrast technique is implemented in the standard Gradient Echo (GE) sequence. A PC-GE sequence is very well suited for straight forward velocity measurements as for cardiac output measurements in the aorta and pulmonary artery [11–13]. However, when extending the acquisition to a full 7D measurement two shortcomings of the technique become prohibitive. The first shortcoming is time. PC-GE uses typically a TR of 10 ms. This seems short, but for a full 7D acquisition this easily adds up to over 40 minutes, which is too long to be of use for clinical practice. The other shortcoming is the signal intensity. In a PC-GE sequence, before applying a new RF-pulse, the net signal from spins that are still in the excited state from the previous pulse is erased by spoiler-gradients (see Figure 1.3 the gradients after read-out). As a result these spins can not contribute to the signal to be created by the new RF-pulse. Therefore, the signal intensity of a PC-GE sequence depends strongly on the inflow of new spins by blood flow into the imaging volume [24, 25]. In case of a 2D image technique with through-plane blood flow, this works properly as blood spends a relatively short time in the image slice. In case of a 3D image of the heart, the situation is completely different. The ventricles act as reservoirs to collect blood, as a result of which blood spends a considerable time in the image volume and signal intensity drops to a level where contrast with the myocardium vanishes [26, 27]. This is shown in Figure 1.6. In summary: PC-GE is less suitable for 7D acquisitions because of its long acquisition time in combination with insufficient contrast and signal intensity.

Steady state sequences, as steady state free precession (SSFP), are often used in CMR because they are fast and have a high signal intensity [26, 28]. The sequence is fast because it does not apply spoiler-gradients but keeps the signal in a steady-state. The signal intensity does not depend so much on inflow of new spins, but depends on the ratio of the T2 and T1 relaxation times which results in a high intrinsic blood-myocardium (heart muscle) contrast (see Figure 1.7). Combination with the phase contrast technique, however, faces some difficulties. In the first place, insertion of the bipolar gradient

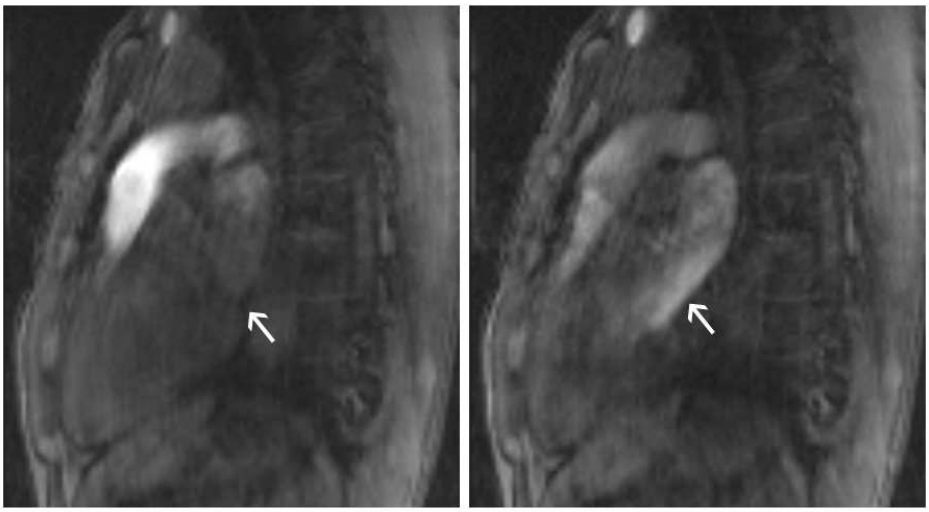

Figure 1.6: 3D PC-GE left in systole and right in diastole. In the left image there is no contrast between the blood and myocardium due to saturation effects, in the right image the contrast of unsaturated spins is clearly visible. The mitral valve is indicated by the white arrows.

causes an increase of TR. Increase of TR makes the steady state more sensitive to disturbance by flowing spins [29–32], resulting in image artifacts. Furthermore, the requirement of phase mapping to subtract two measurements interferes with the preservation of the steady state. Nevertheless, several different implementations have been made by Overall et al. [33], Markl et al. [34], and Pai [35] to incorporate the phase contrast technique in a steady state sequence.

Outline part I

Part I of this thesis evaluates different PC-SSFP sequences on their prospective suitability for quantification of mitral valvular flow. In **Chapter 2** the multiecho method presented by Pai [35] was validated in vitro on a flow phantom and evaluated in vivo on cardiac output measurements in comparison with PC-GE. In **Chapter 3** the approach presented by Overall et al. [33] was implemented in a 3D SSFP sequence. The new sequence was subsequently tested on its

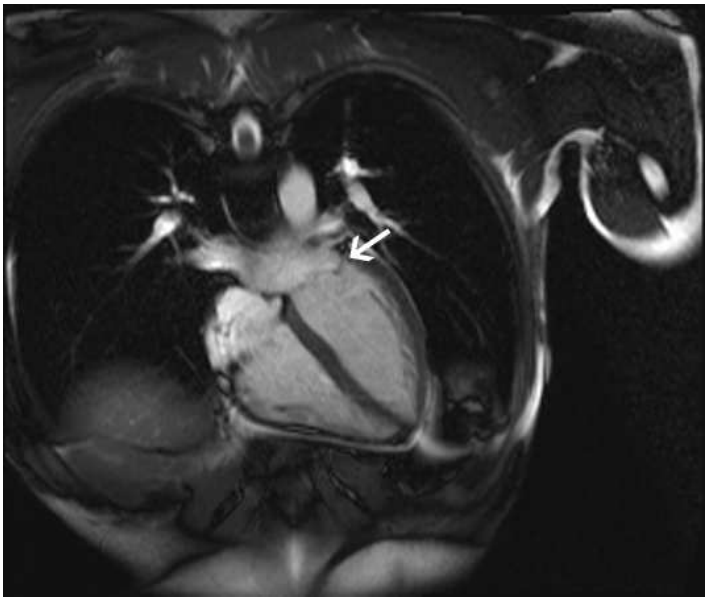

Figure 1.7: Four chamber view using an SSFP sequence showing the high blood-myocardium contrast. The mitral valve is indicated by the white arrow.

imaging and phase mapping properties at the mitral valve. In **Chapter 4** this sequence was further developed to a full 7D PC-SSFP sequence with retrogated cardiac triggering and was tested for mitral valve flow quantification in healthy subjects and patients.

Part II - Velocity Offsets: characterization in a multi-vendor study

Phase signal depends on several phenomena, as was earlier mentioned. The utilized phase signal depends on velocity and the actual gradients. Some of the other phenomena, e.g. local inhomogeneities in the main magnetic field, are constant during the acquisition. These are eliminated by the subtraction of a velocity encoded measurement and a measurement without velocity encoding (in fact, any set of two different velocities will do for this purpose). After subtraction there are, however, two phase phenomena that are uncorrelated to velocity

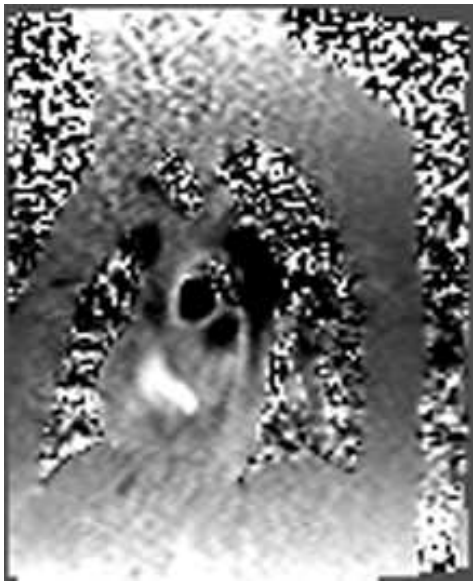

Figure 1.8: Velocity offset from phase differences is shown in the chest wall. The stationary chest wall shows a spatially varying shade of grey. Contrast settings were adapted to show the offset more clearly.

but that do depend on actual gradients and timing. Consequently these phases are non-zero after subtraction. This phase difference translates into a velocity offset that varies spatially over the velocity map, as can be seen in Figure 1.8.

One of the sources of additional phases are the concomitant gradient fields or Maxwell fields. According to Maxwell's laws magnetic field lines form closed loops (zero divergence of the magnetic field). Therefore an isolated linear gradient field cannot be generated, higher order fields will always coexist. But just as these higher order fields are described by Maxwell's law, the resulting phases can be computed and corrected for [36]. A second source of phase effects are eddy currents. Eddy currents are the currents induced in other conducting elements to oppose a changing magnetic field (Lenz's law). In, for example, metal detectors and traffic detection systems eddy currents are used to their advantage. In MR-scanners, however, they are an

unwanted side effect when generating a gradient field and, in contrast to the Maxwell fields, they are not easy to predict and correct for. Eddy currents are compensated for to a large extent (pre-emphasis) [37, 38] and remaining effects have been studied extensively [30, 39–42]. Despite all efforts, the remaining eddy currents can still cause velocity offsets.

In clinical practice these remaining eddy currents can cause large errors in blood flow quantification such as cardiac output measurements. Although the resulting velocity offsets are relatively small (few percent of the v_{enc}), due to the integration over the vessel cross section and over the cardiac cycle the error in flow measurements can become significant (about tenfold). Figure 5.2 on page 91 gives an example of the effect of an offset on aortic flow quantification. Several post-acquisition correction methods exist; the velocity offset can be estimated from static tissue [43, 44]. However, the offset varies with position and in the vicinity of the heart there is no static tissue that can serve this purpose. For cardiac applications an interpolation can be made from static tissue in the chest wall [45, 46]. In all cases, the gold standard is assessment of velocity offsets by an additional phantom acquisition [43]. The eddy currents depend only on the gradients and their timing, they do not depend on the subject/object in the scanner. Therefore a separate scan of a static object, a phantom, can be made to measure correctly the offset as long as the exact same gradients are applied [47].

Outline part II

Existing correction methods work well, as was proved in single center studies. It would however be desirable if a correction could be omitted. Secondly, there is ongoing debate in the field whether this is an individual system performance issue or a broader problem. **Part II** of this thesis studies phase offsets due to eddy currents in a multi-center setting, using protocols comparable to the clinical practice. **Chapter 5** starts off with an investigation of the severity and extent of the offsets among scanners of several vendors. Once the scope of the problem is clear, **Chapter 6** investigates the offset behavior as a function of different protocol parameter settings in order to yield

practical guidelines among vendors for optimization. Existing correction methods assume the background offset to be stable between the time that the velocity acquisition was performed and the correction scan was acquired. In **Chapter 7** this assumption was tested, as there was no published evidence regarding the temporal stability of the phase offsets.

1.5 Bibliography

[1] F. Bloch. Nuclear induction. *Physical Review*, 70(7-8):460–474, 1946.

[2] E.M. Purcell, H.C. Torrey, and R.V. Pound. Resonance absorption by nuclear magnetic moments in a solid. *Physical Review*, 69(1-2):37–38, 1946.

[3] R. Damadian. Tumor detection by nuclear magnetic resonance. *Science*, 171 (3976):1151–1153, 1971.

[4] P.C. Lauterbur. Magnetic-resonance zeugmatography. *Pure and Applied Chemistry*, 40(1-2):149–157, 1974.

[5] A. Kumar, D. Welti, and R.R. Ernst. NMR fourier zeugmatography. *Journal of Magnetic Resonance*, 18(1):69–83, 1975.

[6] P. Mansfield and I.L. Pykett. Biological and medical imaging by NMR. *Journal of Magnetic Resonance*, 29(2):355–373, 1978.

[7] D.J. Pennell, U.P. Sechtem, C.B. Higgins, W.J. Manning, G.M. Pohost, F.E. Rademakers, A.C. van Rossum, L.J. Shaw, and E.K. Yucel. Clinical indications for cardiovascular magnetic resonance (CMR): Consensus pane report. *European Heart Journal*, 25(21):1940–1965, 2004.

[8] C.B. Marcu, A.M. Beek, and A.C. van Rossum. Clinical applications of cardiovascular magnetic resonance imaging. *Canadian Medical Association Journal*, 175(8):911–917, 2006.

[9] J.P. Finn, K. Nael, V. Deshpande, O. Ratib, and G. Laub. Cardiac MR imaging: State of the technology. *Radiology*, 241(2):338–354, 2006.

[10] E.B. Turkbey and D.A. Dombroski. Cardiac magnetic resonance imaging: Techniques and clinical applications. *Seminars in Roentgenology*, 44(2):67–83, 2009.

[11] N.J. Pelc, F.G. Sommer, K.C.P. Li, T.J. Brosnan, R.J. Herfkens, and D.R. Enzmann. Quantitative magnetic-resonance flow imaging. *Magnetic Resonance Quarterly*, 10(3):125–147, 1994.

[12] D.N. Firmin, G.L. Nayler, R.H. Klipstein, S.R. Underwood, R.S.O. Rees, and D.B. Longmore. Invivo validation of MR velocity imaging. *Journal of Computer Assisted Tomography*, 11(5):751–756, 1987.

[13] G.L. Nayler, D.N. Firmin, and D.B. Longmore. Blood-flow imaging by cine magnetic-resonance. *Journal of Computer Assisted Tomography*, 10(5):715–722, 1986.

[14] J. Lotz, C. Meier, A. Leppert, and M. Galanski. Cardiovascular flow measurement with phase-contrast MR imaging: Basic facts and implementation. *Radiographics*, 22(3):651–671, 2002.

[15] W.G. Hundley, H.F. Li, L.D. Hillis, B.M. Meshack, R.A. Lange, J.E. Willard, C. Landau, and R.M. Peshock. Quantitation of cardiac-output with velocity-encoded, phase-difference magnetic-resonance-imaging. *American Journal of Cardiology*, 75(17):1250–1255, 1995.

[16] P.D. Gatehouse, J. Keegan, L.A. Crowe, S. Masood, R.H. Mohiaddin, K.F. Kreitner, and D.N. Firmin. Applications of phase-contrast flow and velocity imaging in cardiovascular MRI. *European Radiology*, 15(10):2172–2184, 2005.

[17] R.O. Bonow, B. Carabello, A.C. de Leon, L.H. Edmunds, B.J. Fedderly, M.D. Freed, W.H. Gaasch, C.R. Mckay, R.A. Nishimura, P.T. O'Gara, R.A. O'Rourke, S.H. Rahimtoola, J.L. Ritchie, M.D. Cheitlin, K.A. Eagle, T.J. Gardner, A. Garson, R.J. Gibbons, R.O. Russell, T.J. Ryan, and S.C. Smith. Guidelines for the management of patients with valvular heart disease - executive summary - a report of the american college of cardiology american heart association task force on practice guidelines (committee on management of patients with valvular heart disease). *Circulation*, 98(18):1949–1984, 1998.

[18] C.M. Tribouilloy, M. Enriquez-Sarano, H.V. Schaff, T.A. Orszulak, K.R. Bailey, A.J. Tajik, and R.L. Frye. Impact of preoperative symptoms on survival after surgical correction of organic mitral regurgitation - rationale for optimizing surgical indications. *Circulation*, 99(3):400–405, 1999.

[19] G. D'Ancona, G. Mamone, G. Marrone, F. Pirone, G. Santise, S. Sciacca, and M. Pilato. Ischemic mitral valve regurgitation: the new challenge for magnetic resonance imaging. *European Journal of Cardio-Thoracic Surgery*, 32(3):475–480, 2007.

[20] K.M.J. Chan, R. Wage, K. Symmonds, S. Rahman-Haley, R.H. Mohiaddin, D.N. Firmin, J.R. Pepper, D.J. Pennell, and P.J. Kilner. Towards comprehensive assessment of mitral regurgitation using cardiovascular magnetic resonance. *Journal of Cardiovascular Magnetic Resonance*, 10, 2008.

[21] L. Sugeng, K.T. Spencer, V. Mor-Avi, J.M. Decara, J.E. Bednarz, L. Weinert, C.E. Korcarz, G. Lammertin, B. Balasia, D. Jayakar, V. Jeevanandam, and R.M. Lang. Dynamic three-dimensional color flow doppler: An improved technique for the assessment of mitral regurgitation. *Echocardiography-A Journal of Cardiovascular Ultrasound and Allied Techniques*, 20(3):265–273, 2003.

[22] L. Sondergaard, F. Stahlberg, and C. Thomsen. Magnetic resonance imaging of valvular heart disease. *Journal of Magnetic Resonance Imaging*, 10(5): 627–638, 1999.

[23] N. Fujita, A.F. Chazouilleres, J.J. Hartiala, M. Osullivan, P. Heidenreich, J.D. Kaplan, H. Sakuma, E. Foster, G.R. Caputo, and C.B. Higgins. Quantification of mitral regurgitation by velocity-encoded cine nuclear-magnetic-

resonance imaging. *Journal of the American College of Cardiology*, 23(4): 951–958, 1994.

[24] J.H. Gao and J.C. Gore. NMR signal from flowing nuclei in fast gradient-echo pulse sequences with refocusing. *Physics in Medicine and Biology*, 39 (12):2305–2318, 1994.

[25] E.M. Haacke, R.W. Brown, M.R. Thompson, and Venkatesan R. *MR Angiography and Flow Quantification*.

[26] K. Scheffler and S. Lehnhardt. Principles and applications of balanced SSFP techniques. *European Radiology*, 13(11):2409–2418, 2003.

[27] R. Nezafat, D. Herzka, C. Stehning, D.C. Peters, K. Nehrke, and W.J. Manning. Inflow quantification in three-dimensional cardiovascular MR imaging. *Journal of Magnetic Resonance Imaging*, 28(5):1273–1279, 2008.

[28] J. Barkhausen, S.G. Ruehm, M. Goyen, T. Buck, G. Laub, and J.F. Debatin. MR evaluation of ventricular function: True fast imaging with steady-state precession versus fast low-angle shot cine MR imaging: Feasibility study. *Radiology*, 219(1):264–269, 2001.

[29] L.B. Hildebrand and M.H. Buonocore. Fully refocused gradient recalled echo (FRGRE): Factors motion sensitivity affecting flow and in cardiac MRI. *Journal of Cardiovascular Magnetic Resonance*, 4(2):211–222, 2002.

[30] O. Bieri and K. Scheffler. Flow compensation in balanced SSFP sequences. *Magnetic Resonance in Medicine*, 54(4):901–907, 2005.

[31] M. Markl, M.T. Alley, C.J. Elkins, and N.J. Pelc. Flow effects in balanced steady state free precession imaging. *Magnetic Resonance in Medicine*, 50 (5):892–903, 2003.

[32] M. Markl. Time resolved three dimensional phase contrast MRI. *Journal of Magnetic Resonance Imaging*, 18(3):396, 2003.

[33] W.R. Overall, D.G. Nishimura, and B.S. Hu. Fast phase-contrast velocity measurement in the steady state. *Magnetic Resonance in Medicine*, 48(5): 890–898, 2002.

[34] M. Markl, M.T. Alley, and N.J. Pelc. Balanced phase-contrast steady-state free precession (PC-SSFP): A novel technique for velocity encoding by gradient inversion. *Magnetic Resonance in Medicine*, 49(5):945–952, 2003.

[35] V.M. Pai. Phase contrast using multiecho steady-state free precession. *Magnetic Resonance in Medicine*, 58(2):419–424, 2007.

[36] M.A. Bernstein, X.J. Zhou, J.A. Polzin, K.F. King, A. Ganin, N.J. Pelc, and G.H. Glover. Concomitant gradient terms in phase contrast MR: analysis and correction. *Magnetic Resonance in Medicine*, 39(2):300–308, 1998.

[37] P. Jehenson, M. Westphal, and N. Schuff. Analytical method for the compensation of eddy-current effects induced by pulsed magnetic-field gradients in NMR systems. *Journal of Magnetic Resonance*, 90(2):264–278, 1990.

[38] J.J. Vanvaals and A.H. Bergman. Optimization of eddy-current compensation. *Journal of Magnetic Resonance*, 90(1):52–70, 1990.

[39] C. Boesch, R. Gruetter, and E. Martin. Temporal and spatial-analysis of

fields generated by eddy currents in superconducting magnets - optimization of corrections and quantitative characterization of magnet gradient systems. *Magnetic Resonance in Medicine*, 20(2):268–284, 1991.

[40] C.B. Ahn and Z.H. Cho. Analysis of eddy currents in nuclear-magnetic-resonance imaging. *Magnetic Resonance in Medicine*, 17(1):149–163, 1991.

[41] Y Zhou, S.D. Wolff, T.M. Grist, and J.A. Polzin. Investigation of eddy current effect on phase contrast imaging. *Proc.Intl.Soc.Mag.Reson.Med.*, 11: 552, 2004.

[42] C. Barmet, N. De Zanche, and K.P. Pruessmann. Spatiotemporal magnetic field monitoring for MR. *Magnetic Resonance in Medicine*, 60(1):187–197, 2008.

[43] A. Caprihan, S.A. Altobelli, and E. Benitezread. Flow-velocity imaging from linear-regression of phase images with techniques for reducing eddy-current effects. *Journal of Magnetic Resonance*, 90(1):71–89, 1990.

[44] Pelc N.J., Herfkens R.J., Shimakawa A., and Enzmann D.R. Phase contrast cine magnetic resonance imaging. *Magnetic Resonance Quarterly*, 7:229254, 1991.

[45] P.G. Walker, G.B. Cranney, M.B. Scheidegger, G. Waseleski, G.M. Pohost, and A.P. Yoganathan. Semiautomated method for noise-reduction and background phase error correction in MR phase-velocity data. *Journal of Magnetic Resonance Imaging*, 3(3):521–530, 1993.

[46] J.W. Lankhaar, M.B. Hofman, J.T. Marcus, J.J. Zwanenburg, T.J. Faes, and A. Vonk-Noordegraaf. Correction of phase offset errors in main pulmonary artery flow quantification. *Journal of Magnetic Resonance Imaging*, 22(1): 73–79, 2005.

[47] A. Chernobelsky, O. Shubayev, C.R. Comeau, and S.D. Wolff. Baseline correction of phase contrast images improves quantification of blood flow in the great vessels. *Journal of Cardiovascular Magnetic Resonance*, 9(4): 681–685, 2007.